Quaternary International 508 (2019) 23–35

Contents lists available at ScienceDirect

Quaternary International

journal homepage: www.elsevier.com/locate/quaint

New insights into the uplifted Roman harbour at Mavra Litharia (N Peloponnese, Greece) in the geodynamic context of the southern margin of the Corinth Gulf

Eleni Kolaiti[a,*], Nikos Mourtzas[b], Konstantinos Kissas[c,f], Fabrizio Antonioli[d], Kurt Lambeck[e]

[a] Geotechnical Engineering Dept, Gaiaergon Ltd, Athens, Greece
[b] Geological Dept, Gaiaergon Ltd, Athens, Greece
[c] Ephorate of Antiquities of Corinth, Corinth, Greece
[d] Laboratorio Modellistica Climatica e Impatti, Centro Ricerche Casaccia, ENEA, Rome, Italy
[e] Research School of Earth Sciences, The Australian National University, Canberra, Australia
[f] Klassische Archäologie FB III, Universität Trier, Trier, Germany

A R T I C L E I N F O

Keywords:
Uplifted Roman harbour
Mavra Litharia
Corinth Gulf
Co-seismic uplift
Palaeogeographic reconstruction
Glacio-isostatic modelling
Vertical tectonic rates

A B S T R A C T

Recent archaeological excavations at Mavra Litharia in the area of Aigeira (N Peloponnese) have brought to light the eastern landward extension of a jetty. The erosion of the cliff along the modern coast and the excavations at the inner side of the northern coastal section of the jetty provided a clearer picture of its structure, significantly different than this presented in previous studies.

The harbour installations are assigned to between the 2nd century and the first half of the 3rd century AD, according to the study of the structure, the mobile findings and the epigraphic data. Biomarkers attached to the structure define the sea level during its operation and demonstrate the current uplift position. The observed damage that has sustained the structure of the ancient jetty suggests that its destruction was co-seismic and reveals the direction of seismic waves from the west. Reconstruction of the displaced blocks of the jetty in their original position, archaeological interpretation and dating of the structure, biomarker information, and glacio-isostatic modelling, determine the sea level since the function of the harbour and the uplift of the ancient jetty as 5.35 ± 0.37 m.

The age of the biological indicators 1686 cal BP (264 AD) is consistent with archaeological dating and the period of the sudden abandonment of the under-reconstruction nearby theatre of ancient Aigeira (mid-3rd century AD). The uplift of the Roman harbour occurred at least in two phases, initially by 4.35 m around 1686 BP and subsequently by 1.0 m around 657 BP.

The mean tectonic uplift rate of 2.81 ± 0.20 mm/yr for the coast in Mavra Litharia, similar to these for the entire western part of the south shore of the Corinth Gulf, is higher than the mean uplift rate of 1.21 ± 0.28 mm/yr in the easternmost edge. The westernmost edge at the Rio-Antirio strait presents very high subsidence rate of 5.17 ± 0.47 mm/yr.

1. Introduction

The 30 m wide, northeast-facing, small cove of Mavra Litharia is located at the central part of the southern coast of the Corinth Gulf (Fig. 1), in the westernmost end of the modern village. Recent archaeological excavations on land revealed the elongated section of a jetty at a distance of 40 m from the current coastline. It is the southeastward continuation of the ruins of a jetty located on the coast. The cove is bordered to the east and west by two conglomerate headlands that enter the sea for around 40 m, consisting of naturally cemented rockfill of the ancient harbour structure. The back beach area is the former harbour basin, filled with post-harbour sediments, forming an elevated platform that is bordered to the west by a hill slope and to the east by the ancient jetty (Fig. 2).

The ancient harbour of Mavra Litharia is one of the few known uplifted harbours in the Eastern Mediterranean. The classical harbour of Falassarna and the Roman breakwater at Kastelli Kissamou, both on the western coast of Crete, were uplifted at +6.60 m during the AD 365

* Corresponding author.
E-mail addresses: kolaitieleni@gmail.com (E. Kolaiti), nikosmourtzas@gmail.com (N. Mourtzas), kkissas@hotmail.com (K. Kissas), fabrizio.antonioli@enea.it (F. Antonioli), Kurt.Lambeck@anu.edu.au (K. Lambeck).

https://doi.org/10.1016/j.quaint.2018.10.020
Received 9 April 2018; Received in revised form 21 July 2018; Accepted 16 October 2018
Available online 17 October 2018
1040-6182/

Fig. 1. Location map of the sites mentioned in the text.

Fig. 2. Aerial view of the study area (image from: https://www.tripinview.com/en/presentation?layer = overview&datasetId = 58007&id = 38719).

earthquake (Pirazzoli et al., 1992; Mourtzas et al., 2016). The harbour of Seleucia Pieria on the coast of SW Turkey in Antioch, dated back to the 4th century BC, rose by a total of 2.50 m in two successive uplifts, around 550 BC and in 526 AD (Erol and Pirazzoli, 1992).

In tandem with the description and interpretation of the ancient harbour installations based on new data from the recent terrestrial archaeological excavations, the present work is aimed at defining the sea level during the operational life of the ancient harbour, at providing evidence of the age of the co-seismic destruction of the harbour installations, at distinguishing the tectonic contribution to sea level change from glacio-isostatic signal, and at reassessing the vertical tectonic rates along the entire southern margin of the Corinth rift.

2. Historical and archaeological context

The ancient city of Aigeira lies on the southern coast of the Corinth Gulf, on Palaeokastro hill, 416 m above sea level. The city was known as 'Hyperesia' during Homeric times until the end of the 7th century BC when it was replaced by Aigeira. It flourished particularly during the Hellenistic and Roman period and was destroyed in the mid-3rd century AD, probably by a strong earthquake (e.g. Gauss et al., 2012). The most important monument of that period was the theatre, which lies 350 m above sea level, north of the Acropolis. The horseshoe-shaped auditorium faced the Corinth Gulf, offering unobstructed and spectacular sea views. The harbour of Aigeira was on the coast, around 1.5 km to the north of the theatre. Pausanias [7.26.1] reported that the harbour bore the same name as the city located within twelve *stadia* from it, and that the coastal town had nothing worth recording. Later on, the location of Mavra Litharia was identified with the ancient harbour of Aigeira (e.g. Walter, 1919; Papachatzis, 1980; Rizakis, 1995; Papageorgiou et al., 1993). The architectural history of the ancient theatre of Aigeira, especially during the last phase of the city when major projects were implemented, seems to follow a parallel course to the construction, the short-lived function, and the destruction of the harbour: founded in the 3rd century BC; undergone small-scale renovations at least three times between the 2nd century BC and the 1st century AD (Gogos, 2001; Gauss et al., 2012); replaced in the 2nd century AD the Hellenistic *proscaenium* by the Roman *scaenae* frons (Alzinger et al., 1986); undergone remodelling in the first half of the 3rd century AD (Gauss et al., 2012); with completion soon interrupted sometime in the mid-3rd century AD (Gogos, 2001). The general political and economic crisis of the empire during this period and its impact on the small city of the northern Peloponnese is not a convincing interpretation for the abandonment of the project, as architectural elements from the theatre were found in a nearby pit ready for calcination. A strong earthquake that could also have caused the first uplift of the harbour looks like a more realistic hypothesis of destruction of the ancient theatre.

3. Geodynamic context

The actively subsiding Corinth rift (Fig. 3) is characterized as one of the most active areas of crustal extension worldwide (e.g. Le-Pichon and Angelier, 1981). The morphologically complex, asymmetrical graben, ca. 130 km long and ca. 30 km wide, reaching a water depth of 900 m in the central part, is bounded by WNW - ESE normal faults, parallel or sub-parallel to the coastline (e.g. Higgs, 1988). The rift is opening at a rate of 11 mm/yr to 16 mm/yr in N–S to NNE – SSW direction (e.g. Collier et al., 1992; Briole et al., 2000; Leeder et al., 2003; Lykousis et al., 2007). It shows higher expansion rates in the western part (15 ± 2 mm/yr) than in the eastern part (10 ± 4 mm/yr) (Clarke et al., 1998; Briole et al., 2000).

Along the south margin of the Corinth rift, the onshore north-dipping faults trend E-W to ESE-WNW in a staircase-like pattern (Doutsos and Poulimenos, 1992; Roberts, 1996), with a visible length ranging between 15 km and 25 km and slip rates 7 mm/yr to 11 mm/yr (Armijo et al., 1996; Stewart, 1996; DeMartini et al., 2004; McNeill et al., 2005). These have caused a vertical displacement up to 3 km and have subdivided the south rift margin into E-W elongate blocks, 5 km–8 km wide and 5 km–10 km long, tilted southwards at 25°–30° (Doutsos and Poulimenos, 1992). The Xylokastro and Eliki faults are the major neotectonic structures of the area and between them is located the Derveni fault, on the footwall of which lies the ancient harbour. The seafloor morphology in the area of Derveni is dominated by the mirror and throw of the fault, as it drops sharply at a depth of around 700 m in a distance of 60 m from the coast (Stefatos, 2005).

Subsidence is observed in the central and northern part of the Corinth Gulf at a rate of 2.5 mm/yr to 3.6 mm/yr (e.g. Briole et al., 2000; Leeder et al., 2003; McNeill and Collier, 2004; Moretti et al., 2004). The south margin of the Corinth rift indicates uplift since the Middle Lower Quaternary at rates that increase westwards (Fig. 3) (e.g. Armijo et al., 1996; Pirazzoli et al., 2004).

Normal faults associate high seismic activity, frequent seismic swarms, and historical devastating earthquakes with a maximum concentration of epicenters in the central and western part of the Gulf. The earthquakes are located in the western part at a depth between 6 km and 11 km, whereas in the eastern part the hypocentral depth is ranging from 4 km to 13 km. Papadopoulos (2000) reported more than 80 historical seismic events within or around the Gulf. During the last 110 years, 10 strong earthquakes greater than 6.2-magnitude and of a

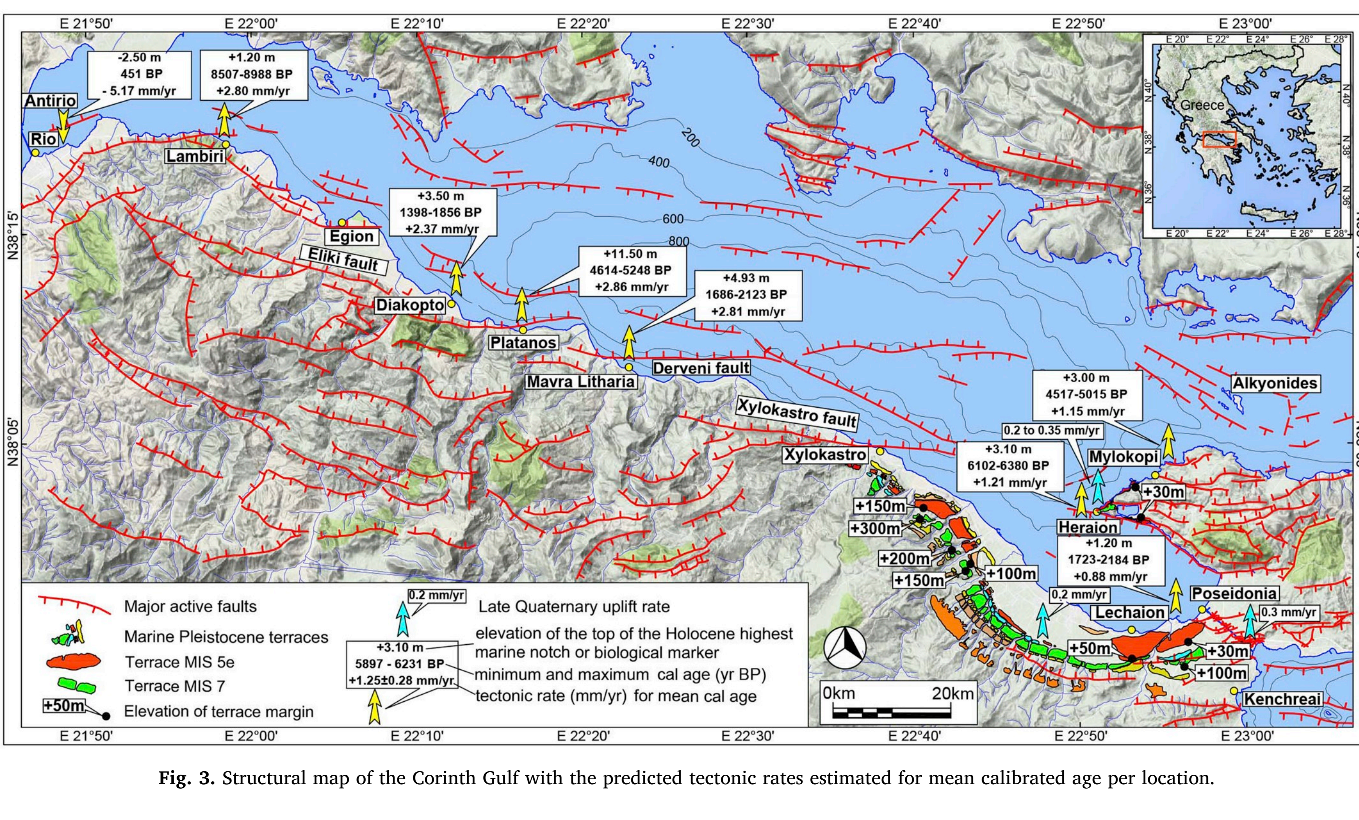

Fig. 3. Structural map of the Corinth Gulf with the predicted tectonic rates estimated for mean calibrated age per location.

shallow focal depth (< 15 km) were reported, the most recent being the 6.2-magnitude earthquake of 1995 that struck Egio (Tselentis et al., 1996; Bernard et al., 2006).

4. Materials and methods

As part of this study the following works have been carried out:

- Archaeological survey and excavation that revealed the eastern landward section of the jetty,
- Topographic survey of the archaeological remains,
- Study of ancient pottery, numismatics and epigraphy,
- Measurement of elevations at characteristic points of the ancient harbour installations,
- Survey of the surficial and underwater morphology of the area,
- Reconstruction in drawings of the displaced blocks of the eastern jetty in order to ascertain their original placement,
- Sampling of fixed biological markers from ashlar blocks of the inner side of the ancient jetty and shells from the sandy basement,
- Radiocarbon ^{14}C dating of fossils,
- Recalibration and correction for reservoir effect of previously obtained radiocarbon ages from the south coast of the Corinth Gulf.

In situ measurements of height at characteristic points of the ancient harbour structure in relation to the present mean sea level were conducted using a topographic instrument (Total Station GPT-3005 LN, TOPCON) and by applying corrections for tide at the time of the survey using data from the Hellenic Navy Hydrographic Service for the closest tide-gauge station at Corinth (Posidonia). The functional height of the jetty was assessed on the basis of archaeological interpretations of the architectural features and the biological mean sea level corresponding to the sampling elevation of the fossils attached to the ancient structure, typical of a former sea level. The archaeological dating of the architectural features of the structure and the mobile findings incorporated into or around it determined the chronological frames of the construction and destruction of the harbour.

The biological mean sea level corresponds to the limit between the infralittoral and midlittoral zones (e.g. Laborel, 1986) and is precisely marked by some species that enjoy very narrow depth ranges located at that limit or a little above or below it (e.g. Stewart and Morhange, 2009). In a protected harbour basin not affected by open sea weather conditions, the measurement error of the biological mean sea level can be only a few centimeters (e.g. Goiran et al., 2009).

The obtained conventional ^{14}C ages that were calibrated using the curve Marine13 and Calib 7.1 software (Reimer et al., 2013; Stuiver et al., 2018) and corrected for the local marine reservoir effect, enabled us to reach the accurate dating of the destruction of the ancient harbour.

The determination of the regional/local marine reservoir effect (MRE) is a key problem for the precise dating of natural disasters that have defined historical events. The local MRE is subject to changes in spatial, temporal and biological factors. In this study we have corrected the conventional ^{14}C ages using a local reservoir age correction value $\Delta R = 133 \pm 75$ yr during the Late Holocene, as suggested by Vött et al. (2018) for the adjacent Lechaion site, some 50 km to the east of the study area, on the southern shore of Corinth Gulf. Vött et al. (2018) have calculated the real local MRE by comparing the conventional ^{14}C ages obtained from marine (sea weed) and terrestrial (wood fragment) samples taken from almost the same depth. The chosen ΔR value is between the two local extrema used in previous studies for the Corinth Gulf: $\Delta R = -80$ yr (Pirazzoli et al., 2004) and $\Delta R = 380$ yr (Soter, 1998).

The tectonic uplift of the harbour area is deduced from the difference between the observed relative sea level, as defined by the height of biomarkers and architectural features of the ancient structure during the function of the harbour, and the predicted relative sea level from the glacio-isostatic modelling in the mean calibrated age.

The glacio-isostatic contribution to sea level change refers to the global response of the earth-ocean system to the growth and decay of the last ice sheets and includes the changing ocean volume, the deformation of the crust, the changes in gravity including the associated geoidal response and centrifugal force. It includes the response to past changes as well as to any recent (centennial and decennial) change in the ice loads. The response is a global one due largely to the redistribution of the melt-water loads and it is an on-going one after the end of deglaciation because of the viscous response of the solid earth to changes in surface loads and internal loads. The theory describing the sea-level response to the changing ice loads is well developed, underpinned by the early work by Peltier (1974) and Farrell and Clark (1976), and the formulation and numerical methods used here have been described in Nakada and Lambeck (1987), Johnston (1993), Lambeck et al. (2003) and is consistent with, but independent off, the theory developed by Mitrovica (2003) and Mitrovica and Milne (2003). In all of these theories the rheological response of the solid earth is as linear viscoelastic with parameters that are determined from the analysis of glacial rebound observations, including sea level. All of these theories also assume no lateral variation in rheological response. The parameters are therefore ‘effective’ parameters intended to describe the response on the time scale of the glacial rebound and for the region being analysed. The other uncertain parameters concern the definition of the ice load. In our models, the ice margins through time are usually assumed known and the ice distribution within these margins in the first instance follow glaciological models that are then tested and modified, iteratively, according to inversions of rebound data separately for the formerly glaciated regions and subject to the requirement that the time function for the total change in ice volume is compatible with the globally averaged change in sea level (Lambeck et al., 2014). This approach has the advantage that it provides a first-order estimate of lateral variation mantle rheology (Lambeck et al., 2017). The ice models used are those of Lambeck et al. (2017).

In the central and eastern Mediterranean region, the sea level isostatic response is about equally distributed between the response to the glacial unloading (glacio-isostasy) (over North America and Fennoscandia) and the response to the changes in water load (hydro-isostasy), primarily that within the Mediterranean basin itself (Lambeck, 1995; Lambeck and Purcell, 2005), yielding a regional ‘short’ wavelength pattern of the basin shape and a ‘long’ wavelength north-northwest to south-southeast trend and it is these variations that permit the estimation of regional ‘effective’ viscosity parameters from observations of sea level change in tectonically (relative) stable regions. The parameters used here therefore are based on outcomes of several regional analyses where the relative importance of the glacio-isostatic and hydro-isostatic components are similar (e.g. Lambeck, 1995, for Greece; Lambeck et al., 2004, for Italy, and Sivan et al., 2001, for Israel). In all these analyses, areas of tectonic stability have been defined as areas where the Last Interglacial sea level is within a few meters of present sea level and where there is no historical or instrumental evidence for vertical movements.

The resulting uncertainties of the predicted isostatic signals will be a function of uncertainties in the ice models, in the choice of earth parameters, and on the adequacy of the definition of relative tectonic stability. We have assessed the three contributions as outlined in Lambeck et al. (2004, see Fig. 2f) using the more recent uncertainty assessments for the global ice-volume function and ice models (Lambeck et al., 2014, 2017) and Mediterranean earth models (Lambeck et al., in prep.). This yield an uncertainty (95% probability) of ~0.20–0.30 m at the epoch of ~2 ka of the Mavra Litharia harbour construction.

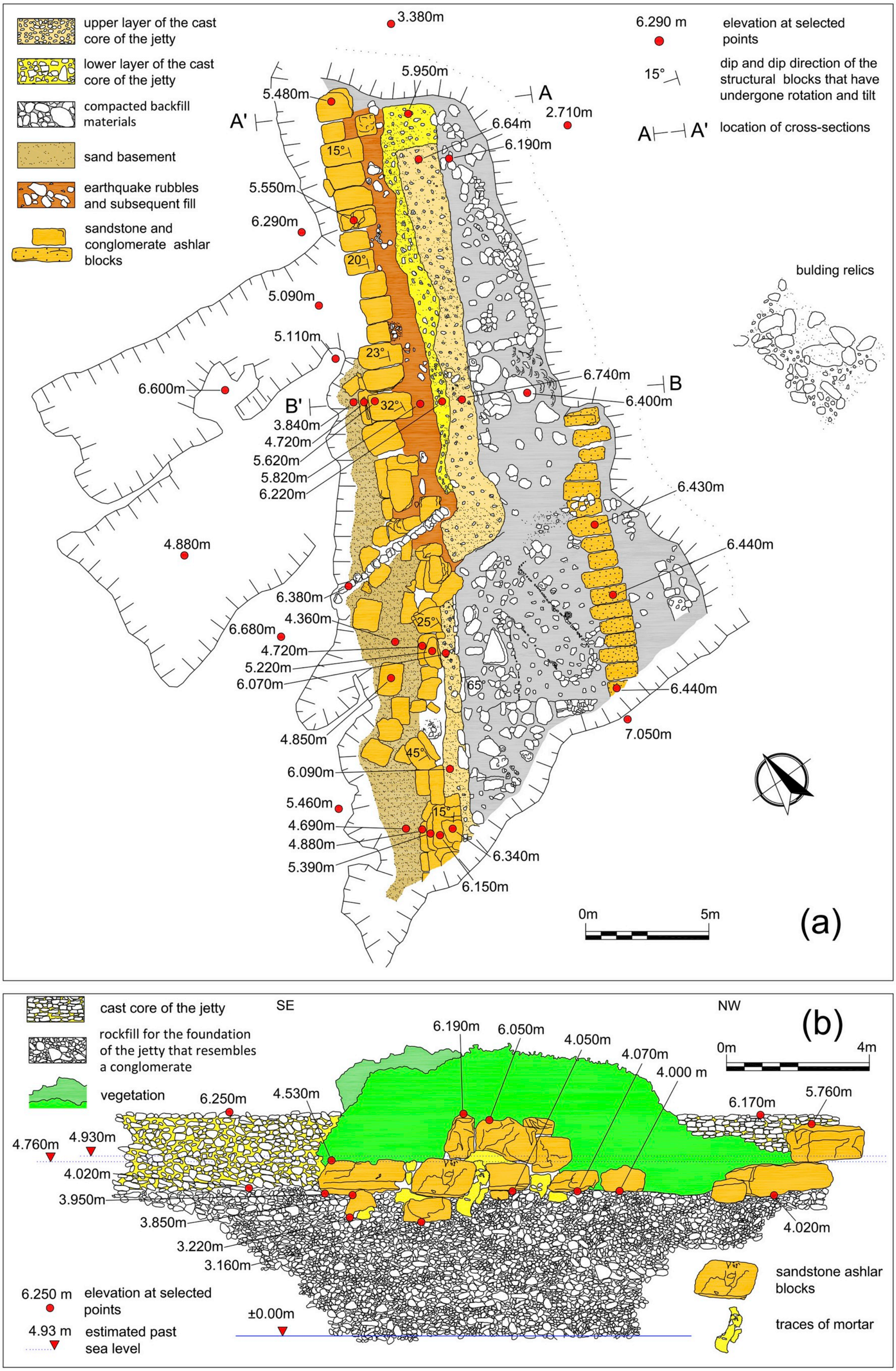

Fig. 4. (a) Plan of the eastern (landward) section of the ancient jetty, (b) Front elevation of the northeastern (coastal) section of the ancient jetty.

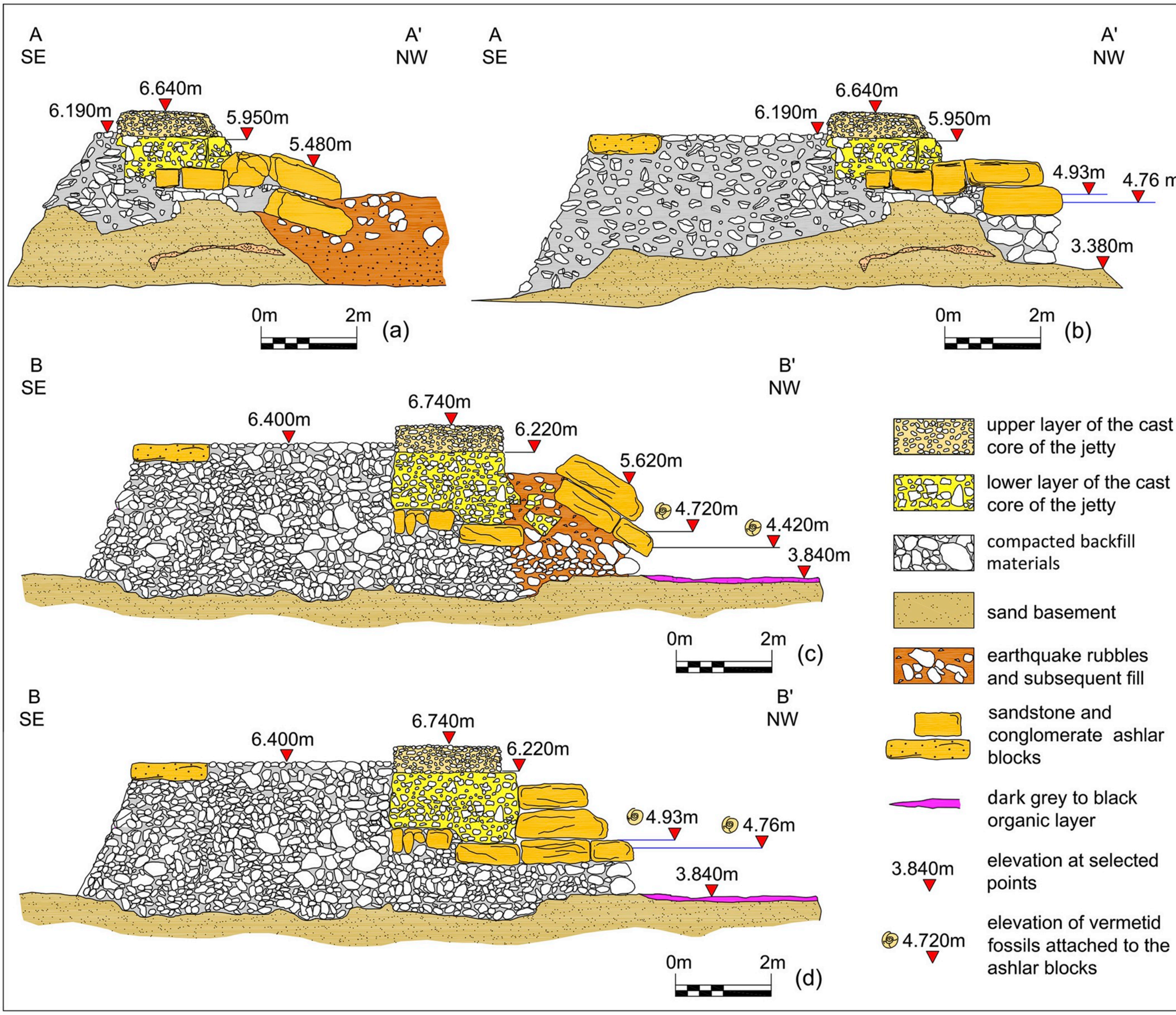

Fig. 5. Cross-sections A-A′ and B—B’ (indicated in Fig. 4a) of the eastern section of the ancient jetty, as it now stands (a, c) and after reconstruction (b, d).

5. Results

5.1. Harbour installations: description and interpretation

The archaeological excavation on land at Mavra Litharia, just above the provincial road between +6.30 m and +7.0 m (all elevations refer to present mean sea level) in a distance of 40 m from the contemporary coastline, has brought to light a jetty, which is the eastern landward section of a harbour structure (Figs. 2, 4 and 8a, b, c, d, e). The coastal sections of the harbour structure lie on both sides of the small cove, but nowadays they are the courtyards of the villas that were built on the filling of the ancient harbour basin (Figs. 2 and 8g, h). Most likely the harbour basin was bounded on the south by a small quarry face (Figs. 2 and 8f), and on the west by a hill slope at the top of which a Roman building has recently been excavated probably related to the harbour installations (Fig. 2).

Eastern (landward) section of the jetty: It is 28 m long, 7 m–11 m wide and consists of a core 18 m long, cast in two layers (Figs. 4a and 8a). It is partly founded on sandstone blocks and partly on compacted backfill materials (Fig. 5a, c). The western toward the basin side of the jetty had been lined with sandstone ashlar blocks, arranged in two to four rows so that the lower course to project by 0.40 m from the upper (Figs. 4a and 5). The blocks were based on backfill materials consisting of sand and pebbles (Figs. 5 and 8e). In the southernmost end of the revealed jetty, a 0.70 m thick retaining wall was constructed to restrain the backfill material (Figs. 4a and 8a, b).

The jetty rests on a sand layer with abundant fossils, which is covered by a 0.10 m dark-grey to black organic layer, found in almost all archaeological pits (Figs. 5 and 8d). This is the bottom of the harbour basin, the depth of which should not exceed 1.50 m. Similar depth has been identified at the inner basins of the Classical harbour of Phalasarna and of the Roman harbour of Lechaion, as well (Hadjidaki, 2001; Mourtzas et al., 2014; Hadler et al., 2013). After the uplift and abandonment of the site, the basin has been filled with roughly 3 m terrestrial deposits that contain many potsherds.

The jetty has sustained damage due to seismic strain released during a large earthquake. The blocks of the western side have moved from their original position by 0.70 m–1.30 m toward the west and have been tilted at 15°–45° toward the west-southwest. The retaining wall in the southernmost part of the jetty has also been tilted at 65° toward the same direction, while cracks and gaps up to 1 m wide are observed in the backfill materials (Figs. 4 and 5a, c, 8a, b, c). Based on the

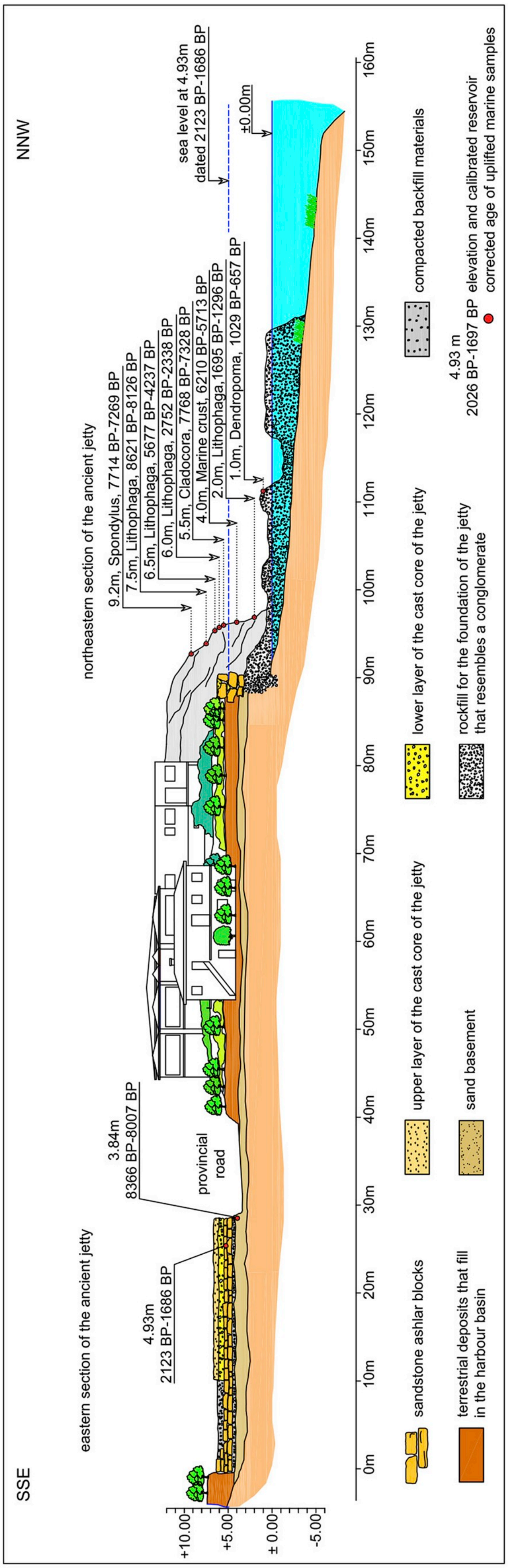

Fig. 6. SSE-NNW cross-section of the study area with the elevations and the calibrated and reservoir corrected ages of the eastern section of the ancient jetty (present study) and of the coral-algal reef, previously dated by Mouyaris et al. (1992), Papageorgiou et al. (1993), Keraudren et al. (1995), Stewart and Vita-Finzi (1996), Stewart (1996) and Pirazzoli et al. (2004).

architectural and constructional features of the jetty, it was possible to reconstruct the displaced blocks of the jetty in drawings and ascertain their original placement (Fig. 5b, d).

Northeastern (coastal) section of the jetty: The erosion of the coastal cliff along the modern coast has revealed the entire stratigraphy of the northeastern section of the jetty up to +6.25 m (Figs. 4b, 6 and 8g). The rockfill for the foundation of the jetty resembles a conglomerate and consists of pebbles naturally cemented together. It reaches the height of +4 m (Fig. 4b) and enters the sea for 40 m up to the depth of −1.50 m (Figs. 6 and 8h). Many potsherds are found attached to its underwater surface (Figs. 6 and 8i). Two courses of sandstone ashlar blocks lie on the seaward side of the rockfill to protect the outer side towards the open sea. A recent rescue archaeological excavation at the southern, toward the basin, side of the jetty revealed one single course of smaller ashlar blocks based on a sand layer with pebbles (Micha, 2009). The cast core, 2.80 m wide and 1.50 m thick, rests on the ashlar blocks and consists of pebbles bound with mortar (Fig. 4b).

The ancient structure has suffered damage in its eastern side along the modern coast and large parts of it were observed underwater. A coastal courtyard wall was constructed subsequently at this position.

Elevations of the harbour structure: The upper surface of the cast core - the highest point of the structure both in the landward (+6.64 m) and in the coastal section (+6.17 m) of the jetty - shows a small difference in elevation of 0.47 m over a distance of 70 m (Fig. 6). The foundation level of the ashlar blocks is almost the same both in the landward (+3.84 m) and in the coastal section (+4.0 m) of the jetty (Fig. 6). The top of the blocks in the eastern landward section of the jetty occurs between +5.48 m and +6.34 m and in the northeastern coastal section between +5.76 m and +6.19 m. These figures suggest that the upper part of the jetty today is dipping toward the north by 2°. The reconstruction in drawings of the displaced blocks of the eastern jetty in their original position, enabled us to understand the function of the ancient harbour structure. We thereupon concluded the functional height of the Roman harbour by considering the elevations of the biological markers attached to it.

5.2. Biological markers - radiocarbon dating

Eight isolate specimens of Vermetus triqueter, typical of the mid-littoral zone, were found attached to the ashlar blocks of the inner side of the jetty (Fig. 7a), almost along the entire length of the eastern landward section, at elevations between +4.42 m and +4.72 m (Fig. 5c), which after the reconstruction of the jetty correspond to original elevations +4.76 m and +4.93 m, respectively (Figs. 5d and 6). The maximum dimensions of the individual shells range from 18 × 15 mm to 21 × 19 mm and the maximum outer whorl diameter is up to 8 mm. Coiling is in counter-clockwise direction (Fig. 7b).

Two fossil samples of marine organisms were collected from the eastern section of the jetty (Figs. 6 and 7). Sample 1 (LTL16761A) consisting of shells (*Chamelea gallina* and *Mactra stultorum*), was collected from the sandy basement at elevation +3.84 m (original elevation: +3.848 m) and yielded a conventional ^{14}C age of 7869 ± 45 BP (calibrated (2σ) and reservoir corrected age using $\Delta R = 133 \pm 75$ yr (Vött et al., 2018) is 8366–8007 yr BP). Sample 2 (LTL16763A), a fixed biological marker *(Vermetus triqueter)* on a sandstone block in the eastern section of the jetty at elevation +4.72 m (original elevation: +4.93 m), yielded a conventional ^{14}C age of 2420 ± 45 BP (calibrated (2σ) and reservoir corrected age is 2123–1686 yr BP) (Table 1).

The calibrated and reservoir corrected ages for sample 2 using $\Delta R = -80$ yr (Pirazzoli et al., 2004) are between 2037 BP (348 BC) and 2297 BP (88 BC), while those using $\Delta R = 380$ yr (Soter, 1998) are between 1499 BP (AD 215) and 1735 BP (AD 415) and, respectively, much older or more recent, than the archaeologically documented age of the construction, function and destruction of the Roman harbour.

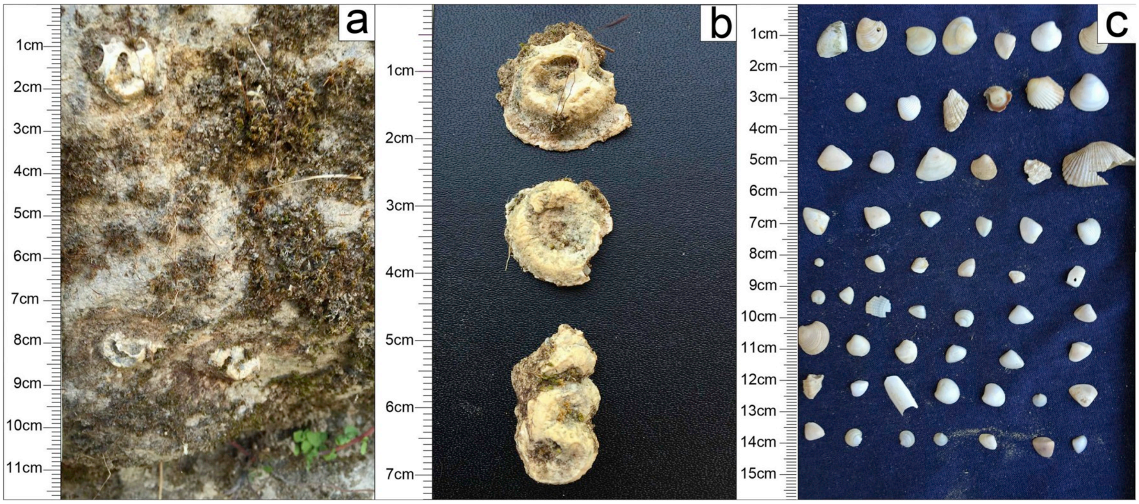

Fig. 7. (a), (b) *Vermetus triqueter* fixed to the ashlar blocks of the inner side of the jetty, (c), (d) bivalves and gastropod molluscs shells from the sand basement.

5.3. Glacio-isostatic modelling

The resulting predicted eustatic-isostatic contributions to sea level change at the epochs of the observed sea level indicators are included in Table 2, with the corresponding uncertainty estimates as given in 'Materials and Methods' section.

Based on data from the Mavra Litharia Roman harbour, we estimated a mean relative sea level change by 4.93 ± 0.20 m during the function of the harbour. Of this, we attribute ~0.25 ± 0.05 m to global sea level rise since ~1800 (Church et al., 2011; Cazenave et al., 2014; Jevrejeva et al., 2014) leaving a tectonic uplift of 5.35 ± 0.37 m with a mean uplift rate of 2.81 ± 0.20 mm/yr, since its construction, co-seismic uplift and destruction (Table 2).

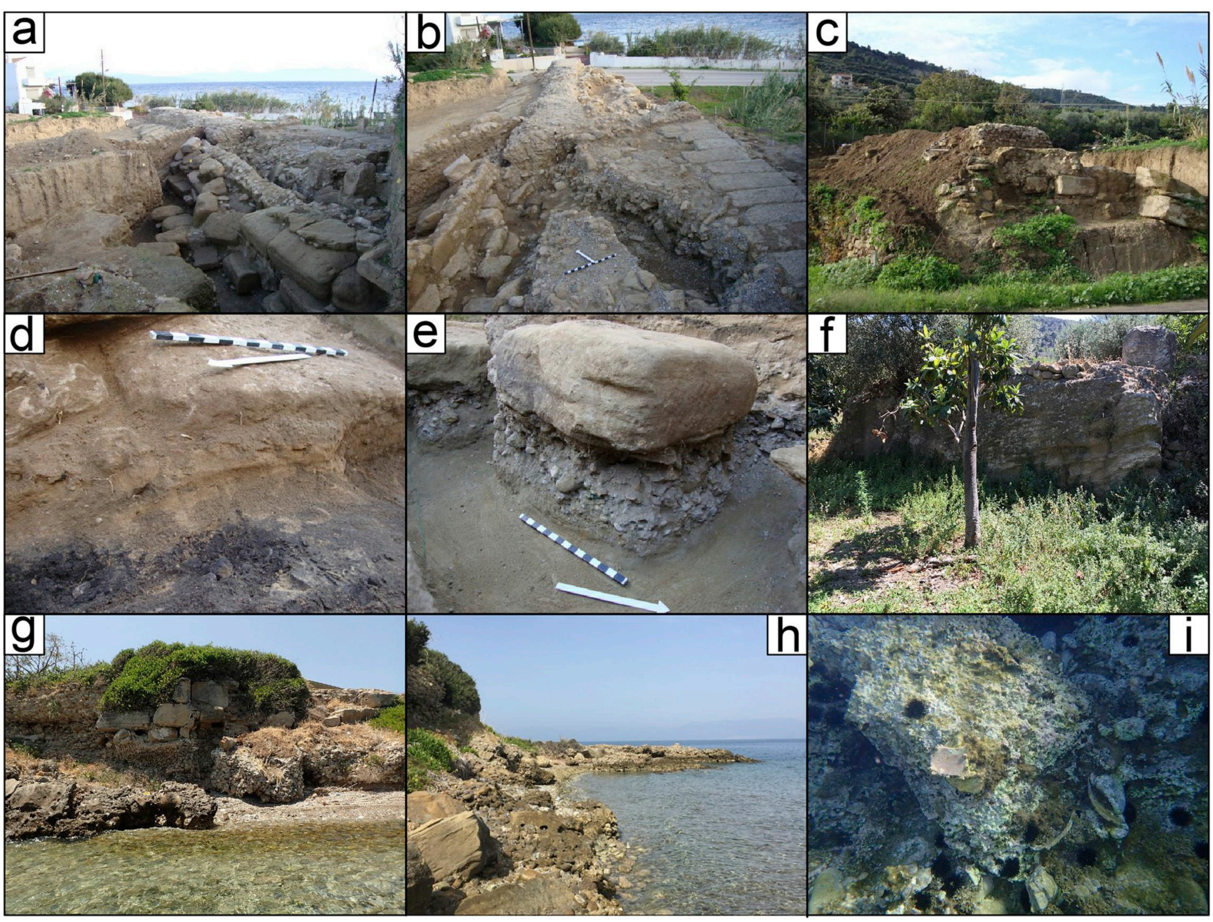

Fig. 8. Views of the eastern landward section of the jetty: (a) the west side that has sustained damage, (b) the upper surface, (c) the northern end, (d) the organic layer that covers the sand basement, (e) foundation layer of the ashlar blocks, consisting of sands and pebbles, (f) quarry face. Views of the northeastern section of the jetty: (g) the structure of the jetty on the coastal cliff, (h) seaward end of the cemented rockfill, (i) underwater view of the cemented rockfill with abundant potsherds incorporated into it and attached to its surface.

Table 1
Radiocarbon ages of mavra litharia harbour (present study).

Sample	Lab. Number	^{14}C age yr BP	(1σ) cal age ranges yr BP	(2σ) cal age ranges* yr BP	(2σ) cal age ranges BC/AD	Elevation (m)	Elevation after reconstruction (m)	Kind of fossil
1	LTL16761A	7869 ± 45	8313–8118	8366–8007	6417–6058 BC	+3.840	+3.848	*Chamelea gallina* *Mactra stultorum*
2	LTL16763A	2420 ± 45	1965–1795	2123–1686	174 BC - 264 AD	+4.720	+4.930	*Vermetus triqueter*

Note: For calibration of ^{14}C ages the calibration curve Marine13 and Calib 7.1 software (Reimer et al., 2013; Stuiver et al., 2018) were used.
*Corrected for local marine reservoir effect ΔR = 133 ± 75 yr (Vött et al., 2018).

6. Discussion

Papageorgiou et al. (1993) were pointed to the very adjacent cove to the west as the Mavra Litharia cove, where they thought that the ancient harbour was located, without providing a description of what they identified as harbour. However, based on the presence of marine conglomerates containing pottery fragments up to +2 m and assuming that these were formed at the bottom of the ancient harbour during or after its period of use and then uplifted, they concluded that the site has undergone a 2 m relative land uplift since Hellenistic times (323–31 BC). Their estimate is at least 3 m lower than our suggestion of 5.35 ± 0.37 m for the uplift of the site and at least 300 yr earlier than our suggestion for the dating of the destruction (264 AD). Based also on *Lithophaga* and *Dendropoma petraeum* fossils exposed up to the elevation of +1 m, they assumed that part of the uplift (1 m at least) was quick, episodic and probably seismic. A conventional ^{14}C age 1420 ± 60 BP was obtained by radiocarbon AMS dating of one single *Dendropoma* fossil (but without providing the exact sampling location and elevation) that yielded a calibrated age of 770–1040 BP and was attributed to the date of the seismic uplift of the site (Papageorgiou et al., 1993). The reservoir age correction of the conventional ^{14}C age 1420 ± 60 BP conducted in this study gave an age 1029 BP - 657 BP (Fig. 6, Table 2), which probably represents an intermediate sea level stand around +1 m, subsequent to the initial uplift of the harbour structure.

Stiros (1998) concluded a relative sea level drop of 4 m, at least 1 m lower than our suggestion of 5.35 ± 0.37 m for the uplift of the site. The suggested date of the harbour uplift (250 AD) was inferred only from archaeological and historical data from the adjacent ancient theatre (Stiros, 1998), without providing any archaeological, geological or radiodating evidence of the harbour site to support his hypothesis. Although Stiros (1998) found neither traces of wood nor pozzolana, he suggested that part of the harbour construction was made with hydraulic cement in a timber mold underwater. Oleson et al. (2004) and Micha (2009) rejected the use of hydraulic cement and *caissons* and suggested the reconsideration of the supposed underwater construction at Mavra Litharia as a rockfill, which is consistent to our observations and interpretation.

Finally, Pirazzoli et al. (2004) dated a marine crust capping the outer rim of a natural cavity at the elevation of +4.0 m, which they erroneously characterized as 'salt pan' related to the sea level at the time of the construction of the ancient Aigeira harbour in the 2nd century AD, 5705 ± 75 ^{14}C years BP (4393–4043 BC or 3960–3520 BC). To explain this discrepancy between the ages of the 'two man-made short-lived constructions' (salt pan and harbour) at about the same elevation (+4 m), they deduced that a relative sea level oscillation should have occurred there. However, this geomorphological feature could not be used as a salt pan as it was at least 1 m below our suggested sea level of 5.35 ± 0.37 m during the operational life of the harbour.

The sand basement with abundant shells that represents the harbour bottom on which rests the eastern section of the jetty, belongs to a sandy terrace, whose calibrated and reservoir corrected age (8366-8007 BP) corresponds to the age of the Holocene coral-algal reef found in Mavra Litharia, around 150 m to the west of the harbour entrance. It is exposed between ca. +4 m and +9.30 m and has been dated by Pirazzoli et al. (2004), yielding recalibrated and reservoir corrected ages between 7714 BP and 5713 BP (Fig. 6, Table 2).

From new robust evidence of the spatial development and the stratigraphy of the harbour structure the functional height of the Roman harbour at +5.35 ± 0.37 m was inferred and the palaeogeographic reconstruction of the Mavra Litharia cove was attempted (Fig. 9). The construction and the operation of the harbour, according to archaeological dating - based on pottery fragments, a stele segment with an inscription, coins, nails, hooks, a bronze medical tool and a small clay figurine unearthed during the recent archaeological excavation at the site - are assigned to between the 2nd century and the first half of the 3rd century AD. The calibrated and reservoir corrected age, obtained from the fixed biological marker on the ashlar blocks of the eastern jetty, between 2123 BP (174 BC) and 1686 BP (264 AD) matches both the archaeological excavation data and the historical evidence of the study area. The age of the abrupt abandonment of the ancient theatre, also coincides with these data. The observed deformation of the structural features of the harbour (displacement and tilt of walls and ashlar blocks toward the west-southwest) indicate a co-seismic tectonic uplift of the Mavra Litharia area.

7. Late Holocene uplift rates for the southern margin of the Corinth rift

The recalibration and correction for reservoir effect of previously published radiocarbon dating, taking into consideration the predicted relative sea level from the glacio-isostatic model, allowed to re-evaluate the age and rate of the Holocene uplift along the entire southern coast of the Corinth Gulf.

Table 2 and Fig. 3 summarize published and new relative sea level data for the southern shore of the Corinth Gulf for sites both to the east (Perachora Peninsula and Lechaion Gulf) and to the west (Lambiri and Rio). In Table 2 are given the original age data, mostly conventional ^{14}C ages along with the calibrated and reservoir effect corrected ages, where appropriate. In Figs. 3 and 6 and in this section the calibrated and reservoir corrected ages are presented. All age uncertainties in ^{14}C calibrated ages (2σ) refer to the original published conventional ^{14}C ages. All elevations given in Figs. 3–6 and Tables 1 and 2 refer to mean sea level. Finally, the observed relative sea level (measured elevations) presented in Table 2 and Fig. 3 refer to the upper limit of the Holocene uppermost marine notch or biological marker. After correction for the glacio-hydro-isostatic effects using the above model, the predicted tectonic rates for mean calibrated age per location are deduced, as presented in Table 2 and Fig. 3.

Based on these data, we conclude that in the central and western section of the southern shore of Corinth Gulf between Mavra Litharia and Lambiri the highest uplift rates are observed, ranging from 2.37 ± 0.19 mm/yr to 2.86 ± 0.29 mm/yr. The extreme west of the Corinth Gulf, at the Rio - Antirio strait, has been submerged by 2.50 m during the last 517 years (451 BP) and demonstrates an extremely high subsidence rate of 5.17 ± 0.47 mm/yr (Kolaiti and Mourtzas, 2016). The easternmost sector of the Corinth Gulf between Lechaion and Mylokopi exhibits the lowest uplift rates, ranging from

Table 2
UPLIFT/SUBSIDENCE rates of the south shore of the Corinth Gulf.

References	Location[a]	Coordinates		kind of indicator/ fossil	^{14}C age[b] (yr BP)	(2σ) cal age ranges[c] (yr BP)		mean cal age (yr BP)	age uncertainty (yr)	observed rsl (elevation) (m)
		Lat (N°)	Long (E°)			min cal age	max cal age			
1	Mylokopi	38°03′23.94″	22°54′37.65″	*Lithophaga*	4705 ± 50	4517	5015	4766	249	+3.00
2	Heraion	38°01′39.78″	22°51′04.56″	*Lithophaga*	5820 ± 60	6102	6380	6241	139	+3.10
3	Lechaion	37°55′55.43″	22°53′10.27″	*Barnacles*	2470 ± 45	1723	2184	1954	230	+1.20
4	Mavra Litharia reef	38°08′26.04″	22°23′02.44″	*Spondylus*	7140 ± 95	7269	7714	7492	222	+9.20
5	Mavra Litharia	38°08′26.04″	22°23′02.44″	*Vermetus triqueter*	2420 ± 45	1686	2123	1905	218	+4.93
6	harbour	38°08′26.04″	22°23′02.44″		1420 ± 60	657	1029	843	186	+1.00
7	Platanos	38°10′29.22″	22°15′31.86″	*Lithophaga*	4800 ± 80	4614	5248	4931	317	+11.50
8	Diakopto	38°11′49.06″	22°12′06.76″	*Lithophaga*	2190 ± 60	1398	1856	1627	229	+3.50
9	Lambiri	38°19′25.54″	21°57′56.04″	*Lithophaga*	8350 ± 50	8507	8988	8748	240	+7.25
10	Rio	38°18′40.26″	21°46′58.70″	Archaeological	–	451		451	–	−2.50

References	rsl prediction[d] (m)			error in observerd rsl[e] (m)	error in isostatic response[f] (m)	RSL change for mean cal age (m)	σ for RSL change[g] (m)	tectonic rate[h] (mm/yr)	σ for tectonic rate[i] (mm/yr)
	min cal age	max cal age	mean cal age						
1	−2.27	−2.67	−2.47	0.28	1.20	+5.47	1.23	+1.15	0.26
2	−4.28	−4.68	−4.48	0.28	1.70	+7.58	1.72	+1.21	0.28
3	−0.49	−0.57	−0.53	0.20	0.33	+1.73	0.39	+0.88	0.20
4	−8.08	−10.10	−9.09	1.03	2.25	+18.29	2.47	+2.44	0.33
5	−0.39	−0.45	−0.42	0.20	0.31	+5.35	0.37	+2.81	0.20
6	−0.22	−0.26	−0.24	0.20	0.08	+1.24	0.22	+1.47	0.26
7	−2.59	−2.60	−2.60	0.20	1.43	+14.10	1.44	+2.86	0.29
8	−0.32	−0.38	−0.35	0.20	0.23	+3.85	0.30	+2.37	0.19
9	−15.91	−18.60	−17.26	1.36	2.81	+24.51	3.12	+2.80	0.36
10	−0.17			0.20	0.04	−2.33[j]	0.21	−5.17[j]	0.47

Note: all decimal numbers are truncated to two decimal places without rounding.

References: 1, 2: Pirazzoli et al. (1994), 3: Morhange et al. (2012), 5: present study, 4, 6, 7: Pirazzoli et al. (2004), 8: Stewart and Vita-Finzi (1996), 9: Palyvos et al. (2008), 10: Kolaiti and Mourtzas (2016).

[a] Locations are indicated in Fig. 1 and 3.

[b] Original uncalibrated published ages.

[c] Original ^{14}C ages were calibrated with calibration curve Marine13 and and Calib 7.1 software (Reimer et al., 2013; Stuiver et al., 2018) and were corrected for local marine reservoir effect $\Delta R = 133 \pm 75$ yr (Vött et al., 2018).

[d] Relarive sea level (rsl) prediction from glacio-isostatic modelling due to age uncertainty only.

[e] Uncertainties from actual elevation measurements and reduction to the present-day mean sea level, uncertainty between the observed quantity and mean sea level and age uncertainty.

[f] Uncertainties from ice- and earth-model parameters.

[g] Includes contributions from all observational and model uncertainties.

[h] Predicted tectonic rate for mean calibrated age.

[i] Uncertainty for tectonic rate for mean calibrated age.

[j] Subsidence.

Fig. 9. Palaeogeographic reconstruction of the ancient harbour of Aigeira at Mavra Litharia cove.

0.88 ± 0.20 mm/yr to 1.15 ± 0.26 mm/yr. All the above Holocene uplift rates are significantly higher than the corresponding rates for the 350 ky and 205 ky BP (Collier, 1990; Collier et al., 1992; Armijo et al., 1996; Dia et al., 1997).

The long-term vertical uplift rates suggested for the eastern part of the south shore of the Corinth Gulf range from 0.30 mm/yr (Dia et al., 1997) to 1.5 mm/yr, due to fault slip rates of 11 ± 3 mm/yr, over the past 350 ky (Armijo et al., 1996). Collier et al. (1992) suggested that the uplift observed at the eastern edge of the Corinth Gulf at a minimum uplift rate of 0.30 mm/yr over the past 205 ky (Collier, 1990) is the result of the regional isostatic uplift above the low-angle subduction under Peloponnese. Leeder et al. (2003) argued that a significant tectonic boundary around the Gulf of Lechaion causes the steep eastward decline in uplift rate towards a zone of no gradient. They also identified a relatively flat-lying lower plate which steepens rapidly under the eastern end of the Gulf causing trench migration forced by southwestward Anatolian plate motion.

This regional tectonic uplift of about 0.2–0.3 mm/yr in the East Corinth Gulf since MIS 7a, can be considered as the background regional tectonic noise. The co-seismic vertical uplift movements occurred during the Holocene, which are related to a tectonic setting of E– W fault zones that cross the north Peloponnesian coast sub-parallel to it, can be regarded as the episodic noise.

8. Conclusions

Sea level during operational life of the ancient harbour is defined at +5.35 ± 0.37 m above present sea level. Radiocarbon dates of the biological markers of between 2123 and 1686 cal. age BP coincide with the archaeological dating of the harbour structure of between the 2nd and the mid-3rd century AD. The damage that has sustained the structure of the ancient jetty suggests that the vertical movement is coseismic and reveals the direction of seismic waves. There is robust evidence that the uplift of the ancient harbour occurred at least in two phases: initially by 4.35 m around 1686 BP (264 AD) and then probably by ~1 m around 657 BP (AD 1300).

The mean tectonic uplift rate on the coast of Mavra Litharia has been estimated as +2.81 ± 0.20 mm/yr. It is one of the higher rates along the entire south coast of the Corinth Gulf, which presents average uplift rates of +1.21 ± 0.28 mm/yr in the extreme east and up to +2.86 ± 0.29 mm/yr in the central and western parts. To the west at the Rio-Antirio strait, extremely high subsidence rate of −5.17 ± 0.47 mm/yr is observed (Kolaiti and Mourtzas, 2016).

Acknowledgements

Special thanks are due to K. Zafeiris, Rural and Surveying Engineer, MSc, who helped us to obtain accurate elevations and to M. Anzidei, PhD, Senior Scientist, INGV, National Earthquake Center, Rome, for the helpful discussions we have had and his valuable remarks. We would like to thank Dr. V. Verrubbi, Paleontologist, ENEA, Casaccia, Laboratorio Modellistica Climatica e Impatti, who helped to identify the fossils. Thanks are also due to Dr S. Furlani, Assoc. Professor, University of Trieste and Mr. D. Aggelou, student of Geology, Kapodistrian University of Athens, for their help during fieldwork. Finally, we would like to thank the anonymus reviewer for the insightful comments and useful suggestions, which helped us to improve the manuscript.

References

Alzinger, W., Gogos, S., Trummer, R., 1986. Aigeira-Hyperesia und die Siedlung Aigeira-Hyperesia und die Siedlung Phelloë in Achaia. Österreichische Ausgrabungen auf der Peloponnes 1972-1983. Teil II. Theater und Umgebung: Klio 68 (1), 5–62.

Armijo, R., Meyer, B., King, P.C.G., Rigo, A., Papanastassiou, D., 1996. Quaternary evolution of the Corinth rift and its implications for the late cenozoic evolution of the aegean. Geophys. J. Int. 126, 11–53.

Bernard, P., Lyon-Caen, H., Briole, P., Deschamps, A., Boudin, F., Makropoulos, K., Papadimitriou, P., Lemeille, F., Patau, G., Billiris, H., Paradissis, D., Papazissi, K., Castarède, H., Charade, O., Nercessian, A., Avallone, A., Pacchiani, F., Zahradnik, J., Sacks, S., Linde, A., 2006. Seismicity, deformation and seismic hazard in the western rift of Corinth: new insights from the Corinth Rift Laboratory (CRL). Tectonophysics 426, 7–30.

Briole, P., Rigo, A., Lyon-Caen, H., Ruegg, C.J., Papazissi, K., Mitsakaki, C., Balodimou, A., Veis, G., Hatzfeld, D., Deschamps, A., 2000. Active deformation of the Corinth rift, Greece: results from repeated global positioning system surveys between 1990 and 1995. J. Geophys. Res. 105 (25), 605–625.

Cazenave, A., Habib-Boubacar Dieng, H.-B., Meyssignac, B., Von Schuckmann, K., Decharme, B., Berthier, E., 2014. The rate of sea-level rise. Nat. Clim. Change 4, 358–361. https://doi.org/10.1038/nclimate2159.

Church, J.A., White, N.J., Konikow, L.F., Domingues, C.M., Cogley, G., Rignot, E.,

Gregory, J.M., Van den Broeke, M.R., Monaghan, A.J., Velicogna, I., 2011. Revisiting the Earth's sea-level and energy budgets from 1961 to 2008. Geophys. Res. Lett. 38, L18601. https://doi.org/10.1029/2011GL048794.
Clarke, P.J., Davies, R.R., England, P.C., Parsons, B., Billiris, H., Paradissis, D., Veis, G., Cross, P.A., Denys, P.H., Ashkenazi, V., Bingley, R., Kahle, H.G., Muller, M.V., Briole, P., 1998. Crustal strain in central Greece from repeated GPS measurements in the interval 1989-1997. Geophys. J. Int. 135, 195–214.
Collier, L.L.E.R., 1990. Eustatic and tectonic controls upon Quaternary coastal sedimentation in the Corinth Basin, Greece. Journal of the Geological Society of London 147, 301–314.
Collier, L.L.E.R., Leeder, M.R., Rowe, P.J., Atkinson, T.C., 1992. Rates of tectonic uplift in the Corinth and Megara basins, central Greece. Tectonics 11, 1159–1167.
DeMartini, P.M., Pantosti, D., Palyvos, N., Lemeille, F., McNeill, L., Collier, R., 2004. Slip rates of the Aigion and Eliki faults from upliftied marine terraces, Corinth Gulf, Greece. Compt. Rendus Geosci. 336, 325–334.
Dia, A.N., Cohen, A.S., O'Nions, R.K., Jackson, J.A., 1997. Rates of uplift investigated through 230Th dating in the Gulf of Corinth (Greece). Chem. Geol. 138, 171–184.
Doutsos, T., Poulimenos, G., 1992. Geometry and kinematics of active faults and their seismotectonic significance in the western Corinth-Patras rift (Greece). J. Struct. Geol. 14, 689–699.
Erol, O., Pirazzoli, P.A., 1992. Seleucia Pieria: an ancient harbour submitted to two successive uplifts. Int. J. Naut. Archaeol. 21 (4), 317–327.
Farrell, W.E., Clark, J.A., 1976. On postglacial sea level. Geophys. J. 46, 79–116.
Gauss, W., Smetana, R., Dorner, J., Eitzinger, P., Latzer-Lasar, A., Leibetseder, M., Trapichler, M., 2012. Old and new observations from the theatre at Aigeira. The architecture of the ancient Greek theatre in acts, international conference at the Danish institute, Athens 27-30 january 2012. In: In: Frederiksen, R., Gebhard, E., Sokolicek, A. (Eds.), Monographs of the Danish Institute at Athens, vol. 17. pp. 267–277.
Gogos, S., 2001. Das Theater von Aigeira. Ein Beitrag zur Chronologie des Zeus-Heiligtums. In: Forschungen in der Peloponnes. Akten des Symposions anläßlich der Feier "100 Jahre Österreichisches Archäologisches Institut Athen", 5.3.-7.3, 1998 V.
Goiran, J.-P., Tronchère, H., Collalelli, U., Salomon, F., Djerbi, H., 2009. Découverte d'un niveau marin biologique sur les quais de Portus: le port antique de Rome. Géoarchéologie de la péninsule italienne: Méditerranée 112, 59–67.
Hadjidaki, E., 2001. The roman destruction of Phalasarna: brit. Arch. Rep. Int. Ser. 940, 155–166.
Hadler, H., Vött, A., Koster, B., Mathes-Schmidt, M., Mattern, T., Ntageretzis, A.K., Reicherter, K., Willershäuser, T., 2013. Multiple late-Holocene tsunami landfall in the eastern Gulf of Corinth recorded in the palaeotsunami geo-archive at Lechaion, harbour of ancient Corinth (Peloponnese, Greece). Z. Geomorphol. 57 (Suppl. 4), 139–180.
Higgs, B., 1988. Syn-sedimentary structural controls on basin deformation in the Gulf of Corinth, Greece. Basin Res. 1, 155–165.
Jevrejeva, S., Moore, J.C., Grinsted, A., Matthews, A.P., Spada, G., 2014. Trends and acceleration in global and regional sea levels since 1807. Global Planet. Change 113. https://doi.org/10.1016/j.gloplacha.2013.12.004.
Johnston, P., 1993. The effect of spatially non-uniform water loads on the prediction of sea-level change. Geophys. J. Int. 114, 615–634.
Keraudren, B., Falgueres, C., Bahain, J.J., Sorel, D., Yokoyama, Y., 1995. Nouvelles datations radiometriques des terrasses marines de Corinthie (Peloponnese septentrional, Grece). Comptes Rendues Acadamie Sciences Paris 320 (2A), 483–489.
Kolaiti, E., Mourtzas, N., 2016. High rates of relative sea level change in the Rio-Antirio strait (Greece) based on archaeological indicators: abstract presented at GeoSUB 2016 Underwater geology. Ustica 58–61 13-17 September 2016.
Laborel, J., 1986. Vermetid gastropods as sea level indicators. In: van de Plaasche, O. (Ed.), Sea Level Research: a Manual for Collection and Evaluation of Data. Geo Books, Norwich, pp. 8–310.
Lambeck, K., 1995. Late Pleistocene and Holocene sea-level change in Greece and south-western Turkey: a separation of eustatic, isostatic and tectonic contributions. Geophys. J. Int. 122, 1022–1044.
Lambeck, K., Purcell, A., 2005. Sea-level change in the Mediterranean Sea since the LGM: model predictions for tectonically stable areas. Quat. Sci. Rev. 24, 1969–1988.
Lambeck, K., Purcell, A., Johnston, P., Nakada, M., Yokoyama, Y., 2003. Water-load definition in the glacio-hydro-isostatic sea-level equation. Quat. Sci. Rev. 22, 309–318.
Lambeck, K., Antonioli, F., Purcell, A., Silenzi, S., 2004. Sea-level change along the Italian coast for the past 10,000 yr. Quat. Sci. Rev. 23, 1567–1598.
Lambeck, K., Rouby, H., Purcell, A., Sun, Y., Sambridge, M., 2014. sea level and global ice volumes from the last glacial maximum to the Holocene. Proceedings of the National Academy of Sciences of USA (PNAS) 111 (43), 15296–15303. https://doi.org/10.1073/pnas.1411762111.
Lambeck, K., Purcell, A., Zhao, S., 2017. The North American Late Wisconsin ice sheet and mantle viscosity from glacial rebound analyses. Quat. Sci. Rev. 158, 172–210.
Le-Pichon, X., Angelier, J., 1981. The aegean sea. Phil. Trans. Roy. Soc. London, Ser A300 357–372.
Leeder, R.M., McNeill, C.L., Collier, E.R., Portman, C.P., Rowe, J.P., Andrews, E.J., Gawthorpe, L.R., 2003. Corinth rift margin uplift: new evidence from Late Quaternary marine shorelines. Geophys. Res. Lett. 30 (12), 1611. https://doi.org/10.1029/2003GL017382.
Lykousis, V., Sakellariou, D., Moretti, I., Kaberi, H., 2007. Late Quaternary basin evolution of the Gulf of Corinth: sequence stratigraphy, sedimentation, fault –slip and subsidence rates. Tectonophysics 440 (1–4), 29–51. https://doi.org/10.1016/j.tecto.2006.11.007.
McNeill, L., Collier, R.E., 2004. Uplift and slip rates of the eastern Eliki fault segment, Gulf of Corinth, Greece, inferred from Holocene and Pleistocene terraces. J. Geol. Soc. London 161, 81–92.
McNeill, L.C., Cotterill, C.J., Henstock, T.J., Bull, J.M., Stefatos, A., Collier, R.E.Ll, Papatheoderou, G., Ferentinos, G., Hicks, S.E., 2005. Active faulting within the offshore western Gulf of Corinth, Greece: implications for models of continental rift deformation. Geology 33 (4), 241–244.
Micha, P., 2009. New data on the seaport of ancient Aigeira at the Mavra Litharia location of western Evrostini. In: In: Kissas, K., Neimeier, W.-D. (Eds.), The Corinthia and the Northeast Peloponnese: Topography and History from Prehistoric Times until the End of Antiquity. Proceeding of the International Conference, Loutraki, 26-29 March 2009, vol. 4. pp. 451–459 Athenaia.
Mitrovica, J., 2003. Recent controversies in predicting post-glacial sea-level change. Quat. Sci. Rev. 22, 127–133.
Mitrovica, J., Milne, G.A., 2003. On post-glacial sea level: I. General theory. Geophys. J. Int. 154, 253–267.
Moretti, I., Lykousis, V., Sakellariou, D., Reynaud, J.-Y., Benziane, B., Prinzhoffer, A., 2004. Sedimentation and subsidence rate in the Gulf of Corinth: what we learn from the Marion Dufresne's long-piston coring. Compt. Rendus Geosci. 336, 291–299.
Mourtzas, N.D., Kissas, C., Kolaiti, E., 2014. Archaeological and geomorphological indicators of the historical sea level changes and the related palaeogeographical reconstruction of the ancient foreharbor of Lechaion, East Corinth Gulf (Greece). Quat. Int. 332, 151–171.
Mourtzas, N.D., Kolaiti, E., Anzidei, M., 2016. Vertical land movements and sea level changes along the coast of Crete (Greece) since Late Holocene. Quat. Int. 401, 43–70.
Mouyaris, N., Papastamatiou, D., Vita-Finzi, C., 1992. The helice fault? Terra. Nova 4, 124–129.
Nakada, M., Lambeck, K., 1987. Glacial rebound and relative sea level variations: a new appraisal. Geophys. J. 90, 171–224.
Oleson, J.P., Brandon, C., Cramer, S.M., Cucitore, R., Gotti, E., Hohlfelder, R.L., 2004. The ROMACONS project: a contribution to the historical and engineering analysis of the hydraulic concrete in Roman maritime structures. Int. J. Naut. Archaeol. 33 (2), 199–229.
Palyvos, N., Lemeille, F., Sorel, D., Pantosti, D., Pavlopoulos, K., 2008. Geomorphic and biological indicators of paleoseismicity and Holocene uplift rate at a coastal normal fault footwall (Western Corinth Gulf, Greece). Geomorphology 96, 16–38.
Papadopoulos, G.A., 2000. A new tsunami catalogue of the Corinth Rift: 373 B.C.–A.D. 2000. In: Papadopoulos, G.A. (Ed.), Historical Earthquakes and Tsunamis in the Corinth Rift, Central Greece, National Observatory of Athens. Institute of Geodynamics, Publ. no 12, pp. 121–126.
Papageorgiou, S., Arnold, M., Laborel, J., Stiros, S., 1993. Seismic uplift of the harbour of ancient Aigeira, Central Greece. Int. J. Naut. Archaeol. 22, 275–281.
Papachatzis, N., 1980. Pausanias' Peregrination of Greece: Details of Achaia and Arcadia, vol. 4. pp. 550p Editions Ekdotike Athenon S.A., Athens.
Peltier, W.R., 1974. The impulse response of a Maxwell Earth. Rev. Geophys. Space Phys. 12, 649–669.
Pirazzoli, P.A., Ausseil-Badie, J., Giresse, P., Hadjidaki, E., Arnold, M., 1992. Historical environmental changes at Phalasarna harbor, west Crete. Geoarchaeology 7 (4), 371–392.
Pirazzoli, P., Stiros, S., Arnold, M., Laborel, J., Laborel-Deguen, F., Papageorgiou, S., 1994. Episodic uplift deduced from Holocene shorelines in the Perachora peninsula, Corinth area, Greece. Tectonophysics 229, 201–209.
Pirazzoli, P.A., Stiros, S.C., Fontugne, M., Arnold, M., 2004. Holocene and Quaternary uplift in the central part of the southern coast of the Corinth Gulf (Greece). Mar. Geol. 212, 35–44.
Reimer, P.J., Bard, E., Bayliss, A., Beck, J.W., Blackwell, P.G., Bronk Ramsey, C., Buck, C.E., Cheng, H., Edwards, R.L., Friedrich, M., Grootes, P.M., Guilderson, T.P., Haflidason, H., Hajdas, I., Hatté, C., Heaton, T.J., Hoffmann, D.L., Hogg, A.G., Hughen, K.A., Kaiser, K.F., Kromer, B., Manning, S.W., Niu, M., Reimer, R.W., Richards, D.A., Scott, E.M., Southon, J.R., Staff, R.A., Turney, C.S.M., der Plicht, J., 2013. IntCal13 and Marine13 radiocarbon age calibration curves 0–50,000 years cal BP. Radiocarbon 55 (4), 1869–1887.
Rizakis, A.D., 1995. Achaie I: Sources textuelles et histoire regionale: Meletemata, v. 20. National Hellenic Research Foundation, Institute of Historical Studies/Department of Greek and Roman Antiquity, Athens, pp. 449p.
Roberts, G.P., 1996. Variation in fault-slip directions along active normal faults. J. Struct. Geol. 18, 835–845.
Sivan, D., Wdowinski, S., Lambeck, K., Galili, E., Raban, A., 2001. Holocene sea-level changes along the Mediterranean coast of Israel, based on archaeological observations and numerical model. Palaeogeogr. Palaeoclimatol. Palaeoecol. 167 (1–2), 101–117.
Soter, S., 1998. Holocene uplift and subsidence of the helike delta, Gulf of Corinth, Greece. In: In: Stewart, I.S., Vita-Finzi, C. (Eds.), Coastal Tectonics, Spec. Publ. Geol. Soc. Of London, vol. 146. pp. 41–56.
Stefatos, A., 2005. Study of Sedimentary Processes and Tectonic Structures in the Corinth Gulf by Using Geophysical Methods. PhD Thesis. University of Patras, Dept. of Geology, pp. 221.
Stewart, I., 1996. Holocene uplift and palaeoseismicity on the Eliki fault, western Gulf of Corinth, Greece. Annals of Geofysics 39 (3), 575–588.
Stewart, I., Vita-Finzi, C., 1996. Coastal uplift on active normal faults: the Eliki Fault, Greece. Geophys. Res. Lett. 23 (14), 1853–1856.
Stewart, S.I., Morhange, C., 2009. Coastal geomorphology and sea-level change. In:

Woodward, J. (Ed.), The Physical Geography of the Mediterranean. Oxford University Press, pp. 385–414.
Stiros, S., 1998. Archaeological evidence for unusually rapid Holocene uplift rates in an active normal faulting terrain: Roman harbour of Aigeira. Gulf of Corinth, Greece: Geoarchaoology 13, 731–741.
Stuiver, M., Reimer, P.J., Reimer, R.W., 2018. CALIB 7.1. at. http://calib.org.
Tselentis, G.-A., Melis, N.S., Sokos, E., Papatsimpa, K., 1996. The egion june 15, 1995 (6.2 ML) earthquake, western Greece. Pure Appl. Geophys. 147, 83–98.
Vött, A., Hadler, H., Coster, B., Matthes-Schmidt, M., Röbke, B.R., Willerschäuser, Reicherter, K., 2018. Returning to the facts: response to the refusal of tsunami traces in the ancient harbour of Lechaion (Gulf of Corinth, Greece) by 'non-catastrophists'-Reaffirmed evidence of harbour destruction by historical earthquakes and tsunamis in AD 69-79 and the 6th cent. AD and a preceding pre-historical event in the early 8th cent. Z. Geomorphol. https://doi.org/10.1127/zfg/2018/0519, 1-28. published online March 2018.
Walter, O., 1919. Ein kolossal kopf des Jeus aus Aigeira. Jahreshefte des Österreichischen Archäol. Inst. Wien 19–20, 1–14.